Energy Conversion and Management 261 (2022) 115642

Contents lists available at ScienceDirect

Energy Conversion and Management

journal homepage: www.elsevier.com/locate/enconman

The case for high-pressure PEM water electrolysis

Ragnhild Hancke *, Thomas Holm, Øystein Ulleberg

Institute for Energy Technology (IFE), P.O. Box 40, Kjeller NO-2027, Norway

ARTICLE INFO

Keywords:
Proton Exchange Membrane Water Electrolysis
PEMEL
Hydrogen compression
Green hydrogen
Techno-economics

ABSTRACT

Hydrogen compression is a key part of the green hydrogen supply chain, but mechanical compressors are prone to failure and add system complexity and cost. High-pressure water electrolysis can alleviate this problem through electrochemical compression of the gas internally in the electrolyzer and thereby eliminating the need for an external hydrogen compressor. In this work, a detailed techno-economic assessment of high-pressure proton exchange membrane-based water electrolysis (PEMEL) systems was carried out. Electrolyzers operating at 80, 200, 350, and 700 bar were compared to state-of-the-art systems operating at 30 bar in combination with a mechanical compressor. The results show that it is possible to achieve economically viable solutions with high-pressure PEMEL-systems operating up to 200 bar. These pressure levels fit well with the requirements in existing and future industrial applications, such as e-fuel production (30–120 bar), injection of hydrogen into natural gas grids (70 bar), hydrogen gas storage (≥200 bar), and ammonia production (200–300 bar). A sensitivity analysis also showed that if the cost of electricity is sufficiently low (<0.1 € kWh^{-1}), it may even be economical to operate PEMEL systems with hydrogen outlet pressures up to 350 bar.

1. Introduction

Green hydrogen from water electrolysis via renewable electricity will be an integral part of the future energy system. In addition to replacing fossil hydrogen as feedstock in existing industries such as ammonia and fertilizer production (currently consuming about 50% of the globally produced hydrogen [1]), green hydrogen is expected to play a central role as an energy vector in emerging markets such as the mobility sector and the renewable power sector [2,3]. Furthermore, green hydrogen may serve as feedstock for e-fuel production and as a reducing agent in steel production [4-8]. Only about 1–2% of the 70 million tones of hydrogen consumed annually is currently produced by renewables [1], but to reach the ambitious European emission targets a significant share of both existing and emerging markets must be served by water electrolysis and renewable electricity in the future.

To efficiently store and transport hydrogen it is necessary to reduce the volume via pressurization or liquefaction. Pressurization of hydrogen to the required end-use pressure is conventionally done by a mechanical compressor, but from an equipment count, process complexity, and plant reliability point of view, pressurizing the gas internally in the electrolyzer is an attractive option [9].

Proton exchange membrane water electrolysis (PEMEL) is well suited for high-pressure operation. Commercial PEMEL systems today operate at hydrogen outlet pressures of 30–40 bar, but prototypes delivering hydrogen at several hundred bar have been demonstrated [10-12]. This is made possible by the solid polymer electrolyte which supports very large pressure gradients across the cells and is contrasted by the alkaline water electrolyzer systems which are limited to balanced pressure operation due to the use of porous separators [13]. Since the pressurization in differential pressure PEMELs is realized electrochemically, no water pressurization pump or balance-of-plant high-pressure components on the oxygen side is required, nor is the handling of compressed oxygen gas. These systems are thus inherently safer, less complex, and produce higher purity gas than balanced pressure electrolyzers.

The major drawback of PEMELs operating under high differential pressures is the comparatively high hydrogen diffusion through the membrane from the hydrogen side to the oxygen side. This decreases the amount of usable hydrogen and therefore the faradaic efficiency of the system. The concentration of hydrogen in oxygen may even exceed the lower flammability limit (LFL) of 4 vol%, making the incorporation of anodic gas recombination catalysts necessary. The other disadvantage is the higher requirements for mechanical strength because the anode cell components receive all the pressure from the cathode side. It may therefore be necessary to use thick or reinforced membranes and porous transport layers, as well as to restrict the size of the active area. This results in higher ohmic losses and may pose a barrier to upscaling.

* Corresponding author.
E-mail address: ragnhild.hancke@ife.no (R. Hancke).

https://doi.org/10.1016/j.enconman.2022.115642
Received 15 December 2021; Received in revised form 1 April 2022; Accepted 13 April 2022
Available online 25 April 2022

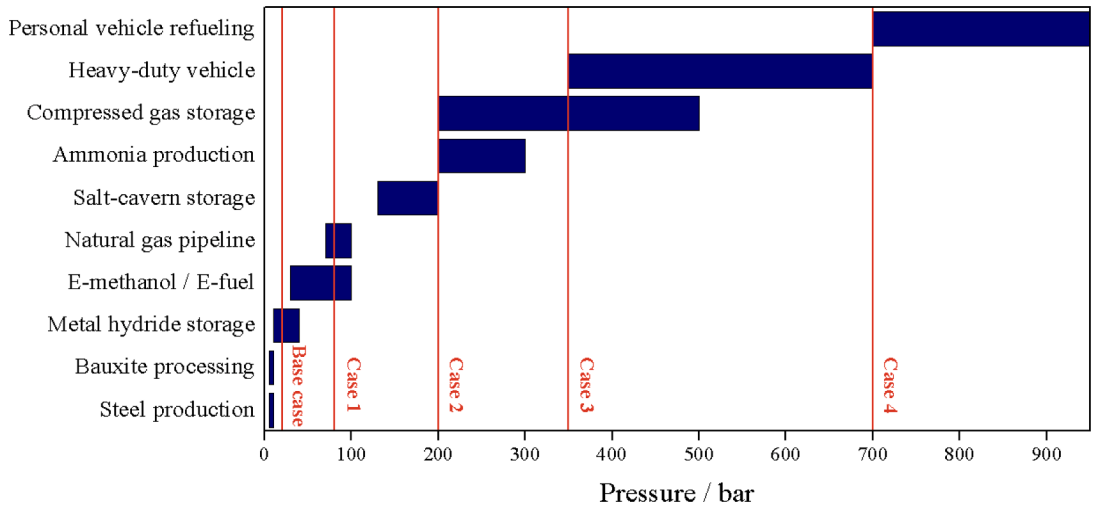

Fig. 1. Existing and future applications for green hydrogen and corresponding pressure levels. The "base case" (30 bar) and the four investigated use cases (80 bar, 200 bar, 350 bar and 700 bar) are indicated.

Table 1
Summary of the evaluated use cases, associated pressures, and relevant applications.

Case	Pressure/ bar	Application
1	80	E-methanol, e-fuels, natural gas pipeline
2	200	Salt-cavern storage, compressed gas storage, ammonia production
3	350	Compressed gas storage, heavy-duty vehicle
4	700	Personal vehicle refueling, heavy-duty vehicle

PEM electrolyzers operating at pressure levels compatible with relevant end-use applications will have several advantages. It will, for example, possible to eliminate the mechanical compressor from the system, replacing a bulky, costly, and noisy component which is prone to breakdown and requires frequent maintenance. In addition to the benefits of reduced system CAPEX and complexity, increasing the electrolyzer pressure makes it possible to increase the plant's capacity or reduce the size of the system components by a factor equal to the pressure ratio. The potential benefit of high-pressure PEM electrolysis has attracted interest academically and in the industry, and has also been the motivation for IFE's research activity on the topic and the establishment of a flexible PEMEL system laboratory for testing of stacks with H_2 outlet pressure up to 200 bar [14].

Examples of existing and future uses of green hydrogen and the corresponding pressure levels are shown in Fig. 1. The low-pressure applications can be served by existing electrolyzer technologies without the use of a mechanical compressor and include metal hydride storage (10–40 bar) [15-17] and metallurgical processes such as steel production (5–10 bar) [4,5,18,19]. The former is attractive for onboard storage in for example trains where the safety requirements are very high and the weight limitations are less strict compared to other transport applications. E-fuel and e-methanol production (requiring a hydrogen stream up to 100 bar) [7,8,20] represent an intermediate pressure application that can benefit from increased electrolyzer operating pressures. An example of this is the ongoing EU project *Djewels* [21] which aims to demonstrate a 20 MW electrolyzer for the production of green methanol using 30 bar alkaline electrolyzers (from McPhy) in combination with mechanical compressors. Injection of hydrogen into the natural gas grid (at ca. 70 bar) [22] is another intermediate pressure use case with large potential: The existing gas grid represents an infrastructure that makes it possible to move large volumes of hydrogen from the generation source to market fast and may thus contribute to accelerate the transition for very large volume users. Ammonia production (200–300 bar) [23] and gaseous storage in salt caverns (130–200 bar) [24,25] or in transport cylinders (180–500 bar) [26] are examples of medium-to-high pressure applications, and so is the onboard tanks in heavy-duty vehicles such as buses, trucks, and ferries (typically at 350 bar). Finally, passenger cars have onboard tanks at 700 bar and require hydrogen refueling pressures up to 950 bar for efficient gas transfer [9,27]. This is thus the application wherein replacing the mechanical compressor will be most challenging.

While many of the applications for green hydrogen listed in Fig. 1 are not economically viable today due to the low cost of grey hydrogen from steam-methane reforming (SMR), they may be realizable in the near future with the expected increase in CO_2 tax and decrease in renewable power and electrolyzer cost [6,9,28,29]. The industrial applications have in addition the benefit of steady demand, meaning that the water electrolysis units can be scaled with the industrial process, and operated regularly at near rated capacity, improving the economics of the overall process. There have been numerous studies on the techno-economic feasibility of water electrolysis-based hydrogen production, e.g., [28,30], but the present study differs from previous work in the field by incorporating a detailed semi-empirical PEMEL cell model (enabling accurate assessment of the effect of changing pressure levels) and focusing on the economic viability of high-pressure systems.

In the study presented in this paper, the techno-economic feasibility of implementing PEM water electrolyzers operating at pressures beyond state-of-the-art technology has been analyzed. Based on the potential markets identified in Fig. 1, four use cases have been investigated and are summarized in Table 1. The electrolyzer pressure states considered are 80 bar, 200 bar, 350 bar, and 700 bar (Cases 1–4, respectively), and these are compared to a reference where the electrolyzer delivers hydrogen at 30 bar and a mechanical hydrogen compressor supplies the gas to the relevant delivery pressure. The main objective of the study is to identify economically viable cases and configurations for high-pressure PEM water electrolysis by answering the following three research questions: i) What is the potential energy- and cost-saving of removing the compressor? ii) What are the optimal conditions and system configuration? iii) Which industry applications are most suitable?

2. Method

A techno-economic modeling tool that can be used to estimate the costs of different designs of water electrolysis-based hydrogen systems on a case-by-case basis has been developed in the program Engineering

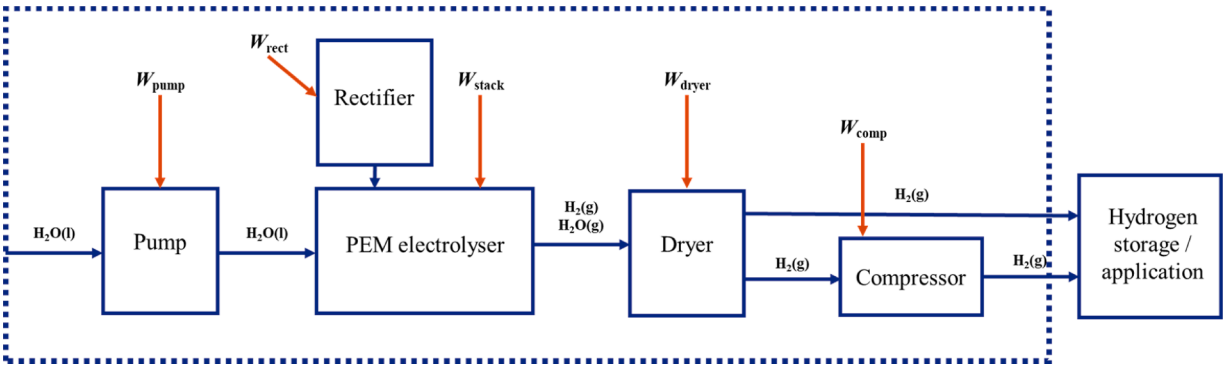

Fig. 2. All the components in the high-pressure PEM electrolyzer setup. The components inside the stippled line are covered by the economic and energetic model.

Equation Solver (EES). The Technical part of the model includes a detailed semi-empirical representation of the electrolyzer stack containing the thermodynamic–, electrochemical- and mass transfer equations necessary to calculate the stack performance. The main equations and empirical coefficients have been taken from literature [13,31-34], and are found in Appendix A. In addition to the PEMEL stack model, the technical model includes terms to account for the parasitic losses of the power supply, the main auxiliary water and gas conditioning systems, and the compressor. The main technical performance parameters (e.g., efficiency and lifetime of components, electrode exchange current densities, and diffusivity of gases in the membrane) and cost functions for the PEMEL stack and key pieces of equipment are entered into the model, in addition to a set of economic parameters (e.g., electricity price, interest rate, project lifetime). From this, the model calculates the system energy demand, the CAPEX and OPEX, and eventually the overall levelized hydrogen cost (€ kg_{H2}^{-1}) for different operating scenarios and cost levels.

2.1. Technical model

A block diagram of the water electrolysis system analyzed is shown in Fig. 2. The components included in the system model are the PEMEL stack (N cells connected in series), the rectifier which supplies the electrolyzer with DC current, the water circulation pump supplying the anode with deionized water at the operating temperature, the H_2 dryer (a chemical adsorption system), and a mechanical compressor. The system work, or the total energy demand per mass net H_2 ($kWh_{elec}\ kg_{H2,net}^{-1}$), is the sum of the work of the stack (W_{stack}), the AC/DC power converter (W_{rect}), the water circulation pump (W_{pump}), the dryer (W_{dryer}) and the mechanical compressor (W_{comp}). In addition, a "miscellaneous" term (W_{misc}) is included to account for the energy usage of auxiliary equipment and processes, e.g., the process parameter measuring devices, the heater which may be used during start-up, and the makeup water pump:

$$W_{tot} = W_{stack} + W_{rect} + W_{pump} + W_{dryer} + W_{comp} + W_{misc} \quad (1)$$

The stack energy use (W_{stack}) can be calculated from the following relation:

$$W_{stack} = \frac{2 \cdot F \cdot U_{stack}}{\eta_F} \cdot f_{loss} \quad (2)$$

Where F is the Faraday constant, U_{stack} is the stack voltage, η_F is the Faradaic efficiency, and f_{loss} represents the H_2 losses related to hydrogen gas management (e.g., dryer regeneration). The stack voltage is a function of operating temperature, pressure, and membrane thickness (δ_m), and is expressed as the sum of the Nernst voltage (U_N) and the kinetic, ohmic, and diffusion overvoltages (U_{kin}, U_{ohm}, and U_{diff}), multiplied by the number of cells in the stack, N:

$$U_{stack} = (U_N + U_{kin} + U_{ohm} + U_{diff}) \cdot N \quad (3)$$

The reader is referred to Appendix A for a detailed description of the different overvoltages. The voltage efficiency (or energy efficiency) of an electrolysis stack is defined as the ratio of the amount of total energy required for splitting one mole of water under reversible conditions (i.e., the thermoneutral voltage U_{tn}) to the actual total amount of energy used in the process (that is, including the energy to overcome irreversibility):

$$\eta_U = \frac{U_{tn}}{U_{stack}} \cdot 100[\%] \quad (4)$$

The Faradaic efficiency represents the fraction of the electric current passing through the electrochemical cell which yields a net H_2 product. It can be expressed as:

$$\eta_F = 1 - \frac{i_{loss}}{i} = 1 - \frac{2 \cdot F \cdot (j_{H_2,loss} + 2 \cdot j_{O_2,loss})}{i} \quad (5)$$

Where $j_{H_2,loss}$ and $j_{O_2,loss}$ are the total crossover fluxes (molar flowrate) of H_2 and O_2 permeated through the polymeric membrane and includes pressure-driven diffusion, concentration-driven diffusion, and diffusion following from water drag (the underlying equations are described in Appendix A).

The Anodic Hydrogen Content (AHC) is the fraction of hydrogen present in the oxygen outlet stream and is usually continuously monitored during operation to ensure that the hydrogen concentration does not reach the LFL. When the hydrogen concentration exceeds, e.g., 50% of LFL (2 vol% H_2), appropriate safety measures should be triggered [34,35]. The AHC is be expressed as:

$$AHC = \frac{j_{H_2,loss}}{\dot{n}_{O_2} + j_{H_2,loss}} \cdot 100 \quad (6)$$

Where $\dot{n}_{O_2}$ (mol $cm^{-2}\ s^{-1}$) is the oxygen production rate which is proportional to the current density (Faraday's law).

The total efficiency of the PEM water electrolysis stack is defined as the product of the Faradaic efficiency and the Voltage efficiency:

$$\eta_{stack} = \eta_U \cdot \eta_F \quad (7)$$

The efficiency of AC-DC power converters is typically greater than 96%, and the energy usage of the rectifier, W_{rect} is accounted for in the model via efficiency curve interpolation [36]. The energy use of the water circulation pump is calculated using the following relation [37]:

$$W_{pump} = \frac{\rho \cdot g \cdot h \cdot q_{H_2O}}{\eta_{pump}} \quad (8)$$

Where ρ represents the water density (kg m^{-3}), g is the gravitational acceleration (m s^{-2}), h is the water head (m), q_{H_2O} is the water flow rate ($m^3\ s^{-1}$), and ρgh corresponds to ΔP_{H_2O} (Pa); the difference between the water inlet pressure and the reference pressure. The water flow rate q_{H_2O} should be adjusted to minimize the temperature difference between the

Table 2
Technical parameters in the model (base case conditions).

Model parameter	Value
Electrolyzer operating temperature, T	60 °C
Electrolyzer H_2 outlet pressure, P_{H2}	30 bar
Electrolyzer O_2 outlet pressure P_{O2}	2 bar
System delivery pressure, P_{del}	700 bar
Current density, i	2 A cm^{-2}
Membrane thickness (N117), δ_m	183 μm
Dryer inlet temperature, T_{Dryer}	30 °C
Dryer loss (of gross H_2), f_{loss}	3% [39]
Dryer regeneration energy, E_{regen}	0.3 kWh_{therm} $mol^{-1}_{H_2O}$ [39]
Dryer efficiency,η_{dryer}	29% [39]
Water pump efficiency,η_{pump}	50% [37]
Miscellaneous load, W_{misc}	0.5 kWh_{elec} $kg^{-1}_{H_2}$ [39]

Table 3
Economic parameters in the model.

Model parameter	Value
Electrolyzer system[a] cost	900 € kW^{-1}_{ely} [42]
Compressor cost	3800 € kW^{-1}_{comp} [47]
Installed electrolyzer system capacity	10 MW
Utilization rate	90%
Lifetime plant	30 years
Lifetime compressor[b]	10 years
Lifetime PEMEL[c]	7 years
PEMEL Degradation rate (μV/h)	3.8 [42]
Discount rate	4%
Site preparation costs (of CAPEX)	5%
Engineering costs (of CAPEX)	10%
Installation costs (of CAPEX)	10%
Contingency (of CAPEX)	5%
Operation & Maintenance costs (of CAPEX)	3%
Energy costs	0.12 € kWh^{-1} [50]
Power costs	30 € kW^{-1} [52]

Notes:
a) Cost of PEMEL stack and BoP (boundary conditions: input of AC power and tap water; output of hydrogen before mechanical compression) [42].
b) Full compressor overhauling after 5000 h of operation. Service costs are assumed to be 20% of compressor CAPEX.
c) Stack replacement cost 35% of electrolyzer system CAPEX [46].

inlet and the outlet (maintain thermal equilibrium) and can be described by the dimensionless lambda factor λ_{H_2O} [38], which is the ratio of the actual water flow rate (q_{H_2O}) to that of the electrolyzed water ($q_{H_2O\rightarrow H_2}$):

$$\lambda_{H_2O} = \frac{q_{H_2O}}{q_{H_2O\rightarrow H_2}} = \frac{2\cdot F}{M_{H_2O}\cdot c^{p}_{H_2O}\cdot \Delta T}(U_{stack} - U_{tn}) \quad (9)$$

where M_{H_2O} is the molar weight of water, $c^{p}_{H_2O}$ is the heat capacity of liquid water at constant pressure, and ΔT is the temperature difference between the stack outlet and inlet.

The energy consumption of the dryer corresponds to the sum of the heat of adsorption, radiation losses, and external heat load to heat the desiccant bed and container. It is proportional to the energy required to regenerate the desiccant, E_{regen} (kWh_{therm} $mol^{-1}_{H_2O}$) and the absolute humidity of the gas, AH (mol_{H_2O} $mol^{-1}_{H_2}$) and can be expressed as:

$$W_{dryer} = AH\cdot E_{regen}\cdot \eta_{dryer}\cdot f_{loss} \quad (10)$$

Based on the analysis carried out by Colella *et al.* [39], we have assumed a regeneration energy, E_{regen}, corresponding to 0.3 kWh_{therm} $mol^{-1}_{H_2O}$ and a dryer efficiency, η_{dryer}, of 3.49 kWh_{elec} kWh^{-1}_{therm}. The absolute humidity of hydrogen as a function of pressure at various saturation temperatures has been taken from Ref. [40].

The required mechanical compressor work is determined based on the assumption of adiabatic compression and calculated from the difference between the delivery pressure and the stack hydrogen outlet pressure:

$$W_{comp} = \left(\frac{\gamma}{\gamma-1}\right)\cdot P_{H_2}\cdot V_0\cdot\left(\left(\frac{P_{del}}{P_{H_2}}\right)^{\frac{\gamma-1}{\gamma}} - 1\right)\cdot\eta^{-1}_{comp} \quad (11)$$

where P_{H_2} is the stack hydrogen outlet pressure (Pa), P_{del} is the delivery pressure, V_0 is the initial specific volume (m^3 kg^{-1}), and γ is the isentropic expansion factor equal to 1.41 for hydrogen at room temperature [35]. The efficiency of hydrogen compressors (electric drive and mechanical efficiency) depends on the compressor type and the number of compression stages, and for diaphragm compressors, a compression ratio of 15 is attainable [41].

Table 2 lists the baseline operating conditions and the input to the technical model in this work. Note that the empirical coefficients which are used to model the cell polarization and the gas crossover are listed in Table A1 in Appendix A. When modeling the PEMEL stack we have assumed the use of a N117 Nafion membrane because this is one of the most widely used membrane for PEMEL systems [35]. We have furthermore assumed that the stack operates at an average of 2 A cm^{-2}, and this corresponds to a load factor of 90% for state-of-the-art systems with a nominal load of 2.2 A cm^{-2} [42].

2.2. Economic model

The economic parameters used in the simulations are listed in Table 3 and include the CAPEX of the PEMEL system and the compressor, the project costs (engineering, site preparation, installation, and contingency), the assumed lifetime of the components, and the PEMEL stack degradation rate. The degradation of a PEMEL stack manifests itself as a slow voltage increase with time and is reported to range between 2 and 5 μV h^{-1} for steady-state operation [43]. The current and projected PEMEL costs have been reviewed in several studies (e.g., [44,45]), showing a relatively large spread of the available CAPEX data for multi-stack systems. In this study, we have therefore chosen to use the electrolyzer system cost provided in the multi-annual work plan of FCH 2 JU (listed as one of the key performance indicators for state-of-the-art PEMEL technology) [42]. It should be noted that this represents the cost of the overall PEMEL system (stack and BoP), and that the stack replacement cost is assumed to be 35% of the initial PEMEL system cost [46].

The compressor cost used in this study (3800 € kW^{-1}) is based on quotations from suppliers of both piston and diaphragm technologies which were collected in connection with Task 33 of IEA's Hydrogen Technology Program and published in Ref. [47]. The cost data are grouped based on different input and output pressures and expressed in relative capital cost as a function of flow rates. The CAPEX of the compressors with input pressure of 5–15 bar and output pressure of 200–300 bar levels out at flow rates above 10 kg h^{-1} and varies between 10 400 € (kg h^{-1})$^{-1}$ and 18 500 € (kg h^{-1})$^{-1}$. The compressors with output pressure of 400–450 bar, on the other hand, have a relative capital cost between 11 100 and 24 900 € (kg h^{-1})$^{-1}$. This translates to costs in the range of 2500–4400 € kW^{-1} and 2300–4900 € kW^{-1} for the two categories, assuming input pressure of 15 bar and output pressures of 300 and 450 bar, respectively. The third category of compressors with input pressure of 200–400 bar and output pressure of 700–1000 bar are less costly (1200–1500 € kW^{-1}). In order to have a proper basis for comparison in this study, the same capital cost has been used for all the considered cases (i.e., inlet pressure of 30 bar, outlet pressure of 80, 200, 350, and 700 bar), and 3800 € kW^{-1} was found to represent the best compromise. However, with such a large spread in quoted compressor costs, there is significant uncertainty associated with this input parameter. This has been accounted for in the sensitivity analysis in section 3.5. Finally, it should be noted that the analysis assumes a compressor service cost of 20% of compressor CAPEX every 5000 hrs. This assumption is based on IFE's experience from operating a hydrogen refueling station at Hynor [48,49] between 2011 and 2016.

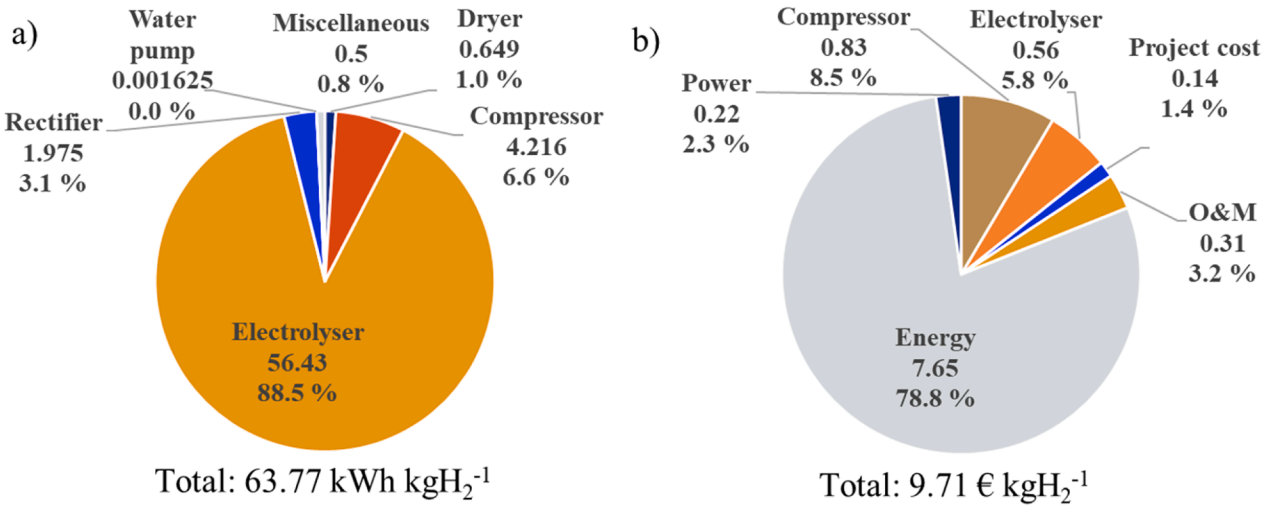

Fig. 3. Distribution of energy (a) and levelized cost of hydrogen (b) for the base case (hydrogen electrochemically compressed to 30 bar followed by mechanical compression to 700 bar).

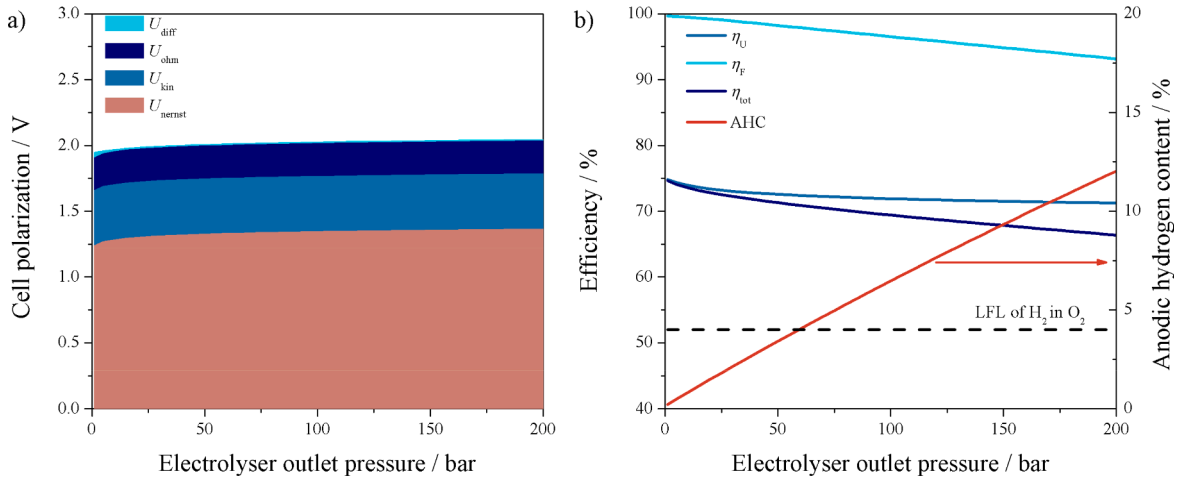

Fig. 4. a) Cell polarization breakdown vs. electrolyzer outlet pressure and b) Electrolyzer cell efficiency and anodic hydrogen content vs. electrolyzer outlet pressure.

The electricity price has been set to 0.12 € kWh^{-1} and corresponds to the average cost for non-household consumers in the EU in 2020 [50]. Today only about 34% of the generated electricity in the EU comes from renewable energy sources [51], but plant owners can ensure that the hydrogen is produced by renewable electricity through power purchase agreements with a Guarantee of Origin. The utilization rate of the electrolyzer is assumed to be 90% (ca 7900 full load hours), i.e., an industrial application with a steady hydrogen demand. It should be noted that this utilization rate is very high compared to a case where the electrolyzer is not grid-connected and instead coupled directly to a variable renewable power source such as onshore wind (typically giving 3200 full load hours) [9]. The power cost utilized in the calculations has been set based on the consumption tariff rate (€ kW^{-1}) for the transmission grid in Norway [52].

The economic model calculates the total CAPEX and OPEX, and eventually, the full levelized cost of hydrogen (LCOH) based on a net present value assessment. The CAPEX includes the project cost (engineering, site preparation, installation, and contingency), the initial PEMEL and compressor investment cost, and the equipment replacement costs. The OPEX includes the operation and maintenance cost and the electricity cost (energy and power). LCOH is derived from the total CAPEX and OPEX over the system lifetime divided by the total hydrogen produced over that lifetime. The calculation is based on the levelized cost of electricity (LCOE), a method that is widely used to compare the unit costs of different renewable energy technologies [3]:

$$LCOH = \frac{\sum_{t=1}^{n} \frac{C_t + O_t}{(1+r)^t}}{\sum_{t=1}^{n} \frac{H_t}{(1+r)^t}} \quad (12)$$

where C_t is the initial investment in year t, e.g. CAPEX, O_t is the operating costs including operations and maintenance costs and the electricity costs, H_t is the annual hydrogen production, t is the number of years, r is the discount rate, and n defines the system lifetime. Different contributions to the levelized costs are calculated in addition to the overall LCOH and will be used in the graphs in the next section:

- The electrolyzer portion of the levelized cost of hydrogen includes the initial PEMEL system investment cost and the stack replacement cost.
- The compressor portion of the levelized cost of hydrogen includes the initial compressor investment cost, the replacement cost, and the service cost.
- The O&M portion of the levelized cost of hydrogen includes the operational and maintenance costs (3% of total CAPEX).
- The project cost portion of the levelized cost of hydrogen includes the site preparation, engineering, installation, and contingency.

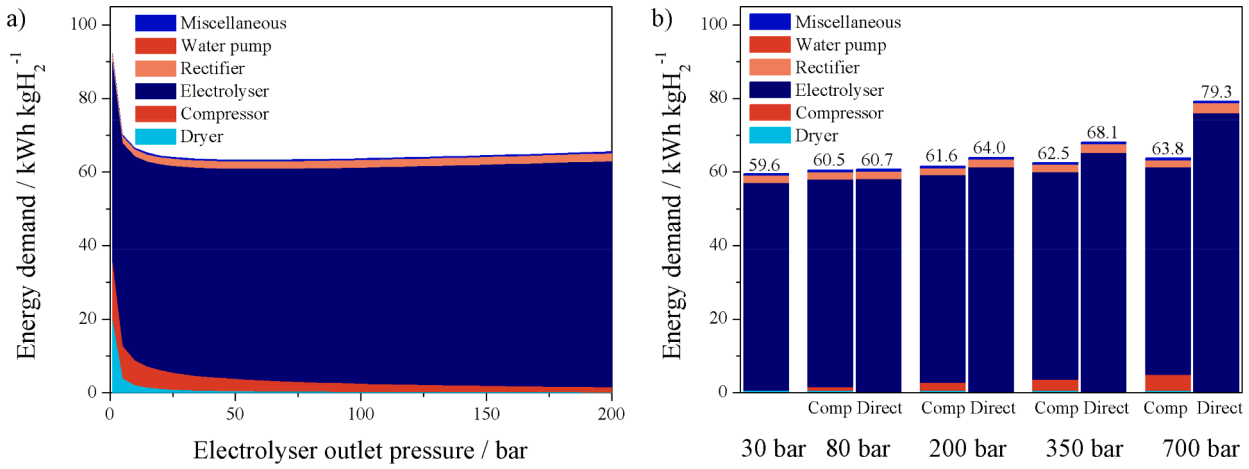

Fig. 5. a) System energy demand as a function of electrolyzer outlet pressure for a final delivery pressure of 700 bar, and b) Comparison of energy demand with mechanical compressor ("Comp") and without ("Direct") for the four considered cases (final delivery pressure of 80, 200, 350 and 700 bar).

- The electricity portion of the levelized cost of hydrogen accounts for the energy cost and the consumption tariff rate for the transmission grid.

3. Results and discussion

3.1. Energetic and economic cost breakdown of state-of-the-art PEMEL (base case)

The base case scenario in this study describes a 10 MW PEMEL system where hydrogen is produced at 30 bar and then compressed mechanically to 700 bar. The installed capacity of 10 MW corresponds to a production rate of 4044 $kgH_2\ day^{-1}$ at the beginning of life and requires compressor power of about 800 kW to take the 30 bar stream from the electrolyzer up to a delivery pressure of 700 bar. On the cell level, operating the electrolyzer under the conditions listed in Table 2 corresponds to a cell voltage of 1.97 V, a voltage efficiency (HHV) of 73.3%, and a Faradaic Efficiency of 98.9%. The distribution of system energy and levelized cost of hydrogen is shown in Fig. 3.

The total energy demand (Fig. 3a) is 63.77 kWh kgH_2^{-1}, and as expected, the largest part comes from the electrolyzer (88.5%), comparable with what is commonly reported [28]. Other major contributions to the system energy demand are the compressor (6.6%), rectifier (3.1%), and dryer (1.0%). While the rectifier, water pump, and "miscellaneous" electrical loads are largely unavoidable and independent of the electrolyzer H_2 outlet pressure, the compressor and dryer energy demands can be reduced by increasing the pressure (shown in Fig. 5).

The total levelized cost of hydrogen delivered at 700 bar is 9.71 € kgH_2^{-1} in this analysis. The LCOH breakdown is provided in Fig. 3b) and shows how the cost is dominated by the electricity cost, where the energy cost makes up 78.8% and the power cost 2.3%. The rest of the costs are related to the electrolyzer CAPEX (5.8%), hydrogen compressor CAPEX (8.5%), operation and maintenance costs (3.2%), and the project cost (1.4%). Reducing or removing the power cost (i.e., the grid connection fees) has been discussed as an approach to accelerate the deployment of green hydrogen, but the cost breakdown in Fig. 3 shows how little effect this will have if the energy costs are as high as the 2020 average EU rate.

It should be noted that the full compressor overhaul after 5000 h operation at a service cost of 20% of the compressor CAPEX has a considerable impact on the compressor contribution to the LCOH. Sensitivity analysis shows that the compressor contribution would be reduced from 0.83 € kgH_2^{-1} to 0.24 € kgH_2^{-1} for the base case by removing this assumption.

3.2. Performance of high-pressure PEMEL stacks

In Fig. 4a) the cell polarization (calculated according to the model presented in Appendix A) is plotted as a function of electrolyzer H_2 outlet pressure, indicating the individual cell voltage contributions to the overall polarization. Theoretically, the electrochemical compression loss in a PEM electrolyzer can be predicted by the Nernst Equation, adding 55 mV to the cell voltage going from 30 to 200 bar at 60 °C (differential pressure). The mass transport polarization decreases slightly with pressure, but at 2 A cm^{-2} this has a marginal impact on the cell voltage as the overvoltage contribution is only 12.3 mV at 30 bar and 10.5 mV at 200 bar. It has also been proposed that high-pressure operation increases the ohmic [53] losses and decreases the kinetic [54] losses, but these interrelations have not yet been validated and have therefore not been included in the electrochemical model used in this study.

Figure 4b) shows the evolution of the voltage efficiency, the Faradaic efficiency, the total efficiency, and the anodic hydrogen content (AHC) as a function of electrolyzer outlet pressure. The voltage efficiency (relative to the higher heating value HHV) decreases from 75% at atmospheric pressure to 71% when the outlet pressure increases to 200 bar, while the Faradaic efficiency decreases from 100% to about 90% due to the enhanced hydraulic driving force for hydrogen back-diffusion across the membrane. From Fig. 4b), it can also be seen that the lower flammability limit (LFL) of H_2 in O_2 is exceeded at a H_2 outlet pressure of 60 bar when the electrolyzer is operated at 2 A cm^{-2}. This underscores the need to implement mitigating measures such as a thicker membrane or a recombining catalyst at the anode if the system utilizing a N117 type of membrane is to face differential pressures above 60 bar. The overall electrolyzer efficiency, which is the product of the Faradaic and the voltage efficiency, decreases from 75% at atmospheric pressure, to 66% at a differential pressure of 200 bar.

3.3. Energetic and economic cost breakdown of high-pressure PEMEL systems

Even though at the cell level, internal pressurization requires more energy than unpressurized electrolysis, increasing the electrolyzer pressure can be energetically favorable from a system perspective since it will reduce the energy demand for both the mechanical compression and the gas drying process. The latter is related to the change in absolute humidity. The absolute humidity of hydrogen fully saturated with water at 30 bar is about 11.8 $gH_2O\ gH_2^{-1}$ (equivalent to a drying energy demand of 0.65 kWh kgH_2^{-1}), which decreases to only about 1.8 gH_2O gH_2^{-1} (drying energy demand of 0.10 kWh kgH_2^{-1}) at 200 bar [40]. The

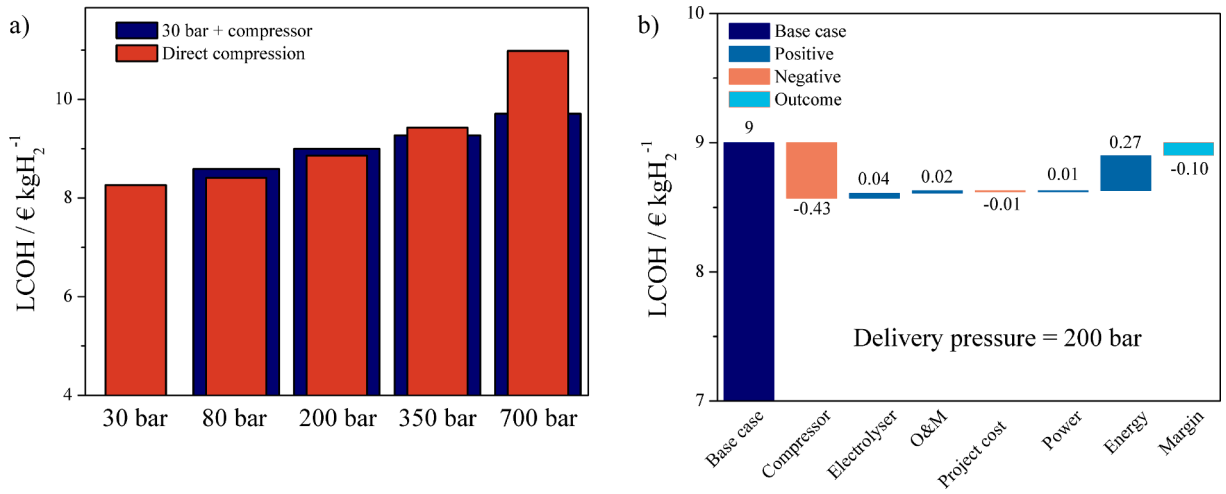

Fig. 6. a) LCOH at different end-use pressures. The cost of a 30 bar-system in combination with a mechanical compressor is compared to the cost of a system with only electrochemical compression for each case. b) The added, subtracted and net change in LCOH when moving from a 30 bar PEMEL system in combination with a compressor to one operating at 200 bar.

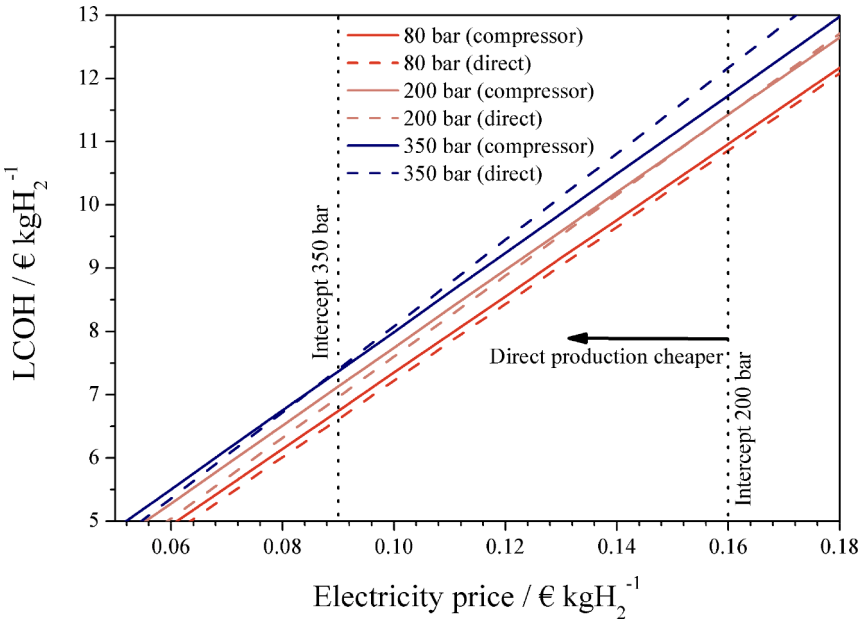

Fig. 7. The cost of hydrogen for Case 1 (80 bar), Case 2 (200 bar) and Case 3 (350 bar) plotted as a function of electricity price. The intercepts indicate the electricity price thresholds below which electrochemical compression may become economically viable.

energy requirement of the mechanical compressor decreases from 4.22 to 1.37 kWh kgH_2^{-1} when the electrolyzer outlet pressure increases from 30 to 200 bar (final delivery pressure of 700 bar).

The overall system energy demand is plotted as a function of electrolyzer outlet pressure for a final delivery pressure of 700 bar in Fig. 5a). The lowest overall energy demand is found at an electrolyzer outlet pressure of 60 bar, similar to the conclusion by Bensmann *et al.* [55] who investigated the optimal configurations of water electrolysis plants. Tjarks *et al.* [56] carried out similar analyses and suggested that the optimal delivery pressure at 2 A cm^{-2} is about 15 bar. Pressurized operation and the associated optimum is expected to be system-specific and depend on each business case and application, but generally, the trade-off is assumed to sit somewhere between 30 and 70 bar [9].

In Fig. 5b) the overall PEMEL system energy demand for the four considered Cases (final delivery pressures of 80, 200, 350, and 700 bar) are shown. Systems with only electrochemical compression are compared to systems with electrochemical compression to 30 bar followed by mechanical compression. The results show that in all of the cases the system energy demand is higher with direct electrochemical compression than when electrochemical and mechanical compression is combined. The difference is 0.22, 2.33, 5.57 and 15.48 kWh kgH_2^{-1} at 80, 200, 350 and 700 bar, respectively.

Despite the increased energy cost of internal pressurization, water electrolysis at the pressure levels compatible with the end-use applications identified in Fig. 1 and Table 1 may be economically viable because the compressor cost represents a significant share of the overall hydrogen cost. A bar chart of the levelized cost of hydrogen at different end-use pressures is shown in Fig. 6a). For each use case, the cost of a 30 bar system in combination with a mechanical compressor is compared to the cost of a system with only electrochemical compression. Notably the CAPEX of the PEMEL system will increase when going to higher pressures, but since the magnitude of this cost increase is unknown, the PEMEL CAPEX is assumed unchanged in order to explore the boundary conditions for which pressurized operation can be beneficial.

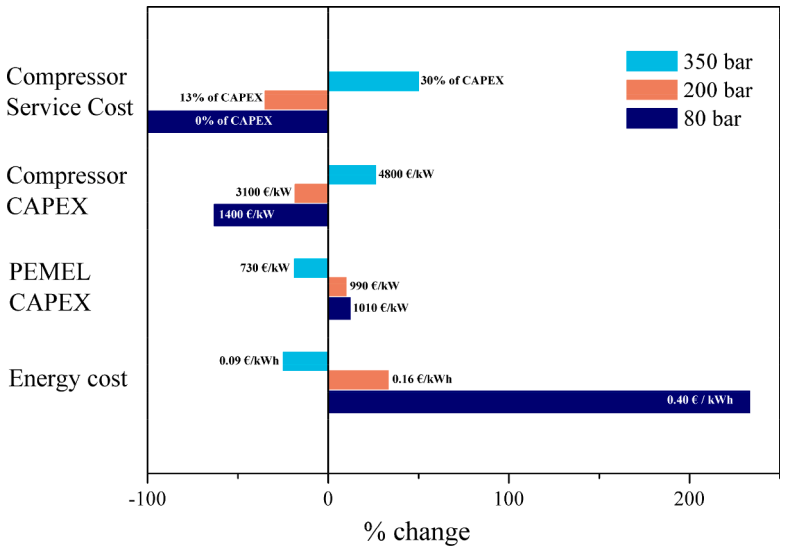

Fig. 8. Sensitivity analysis showing the needed change in cost parameters to reach parity between direct compression and mechanical compression for use cases 1–3 (80, 200 and 350 bar). Direct compression is taken as the zero point (solid black line).

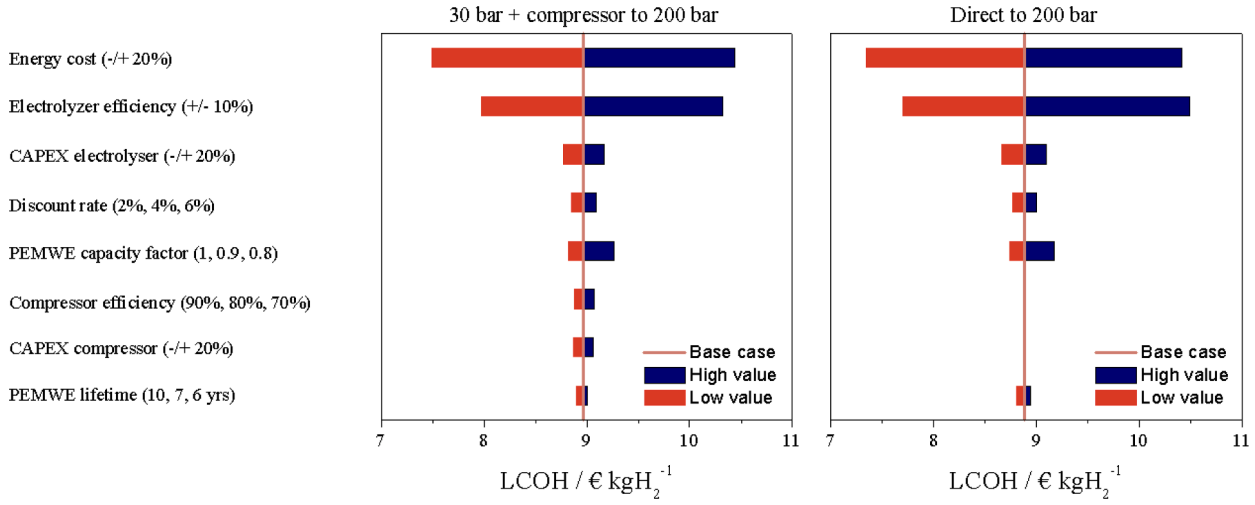

Fig. 9. The sensitivity of the LCOH to changes in the various input parameters for Case 2 (200 bar).

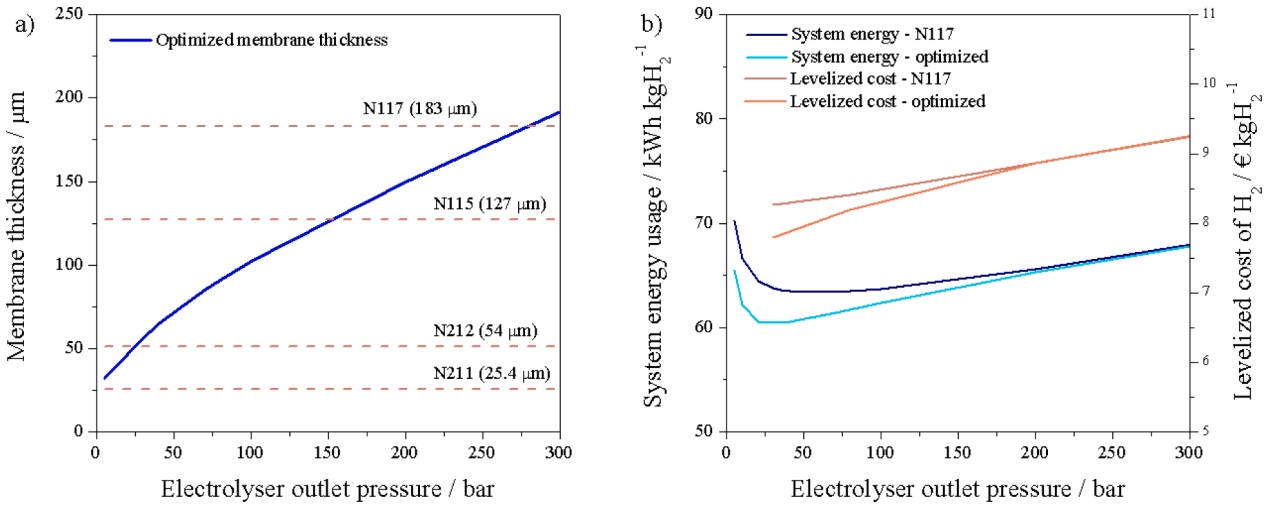

Fig. 10. a) Energetically optimal membrane thickness vs. electrolyzer outlet pressure at a final delivery pressure of 700 bar. The commercial Nafion type of membranes are indicated. b) overall system energy use and LCOH vs. electrolyzer outlet pressure compared for N117 and optimal membrane thicknesses.

Figure 6a) shows that it may be economically feasible to implement PEMELs with 80 and 200 bar outlet pressure, as the LCOH in these two cases is reduced by 0.18 and 0.10 € kgH_2^{-1}, respectively (compared to the case with a separate compressor). These cost differentials translate to a PEMEL CAPEX difference of about 110 EUR kW^{-1} for an 80 bar system and 90 EUR kW^{-1} for a 200 bar system. This is equal to the maximum cost penalty that can be allowed for the high-pressure PEMEL system to be on par with 30 bar systems in combination with a compressor. However, it should here be noted that these cost penalty thresholds are highly dependent on the cost of electricity, as discussed in more detail below. At 350 and 700 bar, direct compression will not be viable in this example.

An illustration of how removing the compressor affects the LCOH is provided for Case 2 (200 bar) in the waterfall chart in Fig. 6b). A significant cost reduction is realized by removing the mechanical compressor CAPEX, but at the same time, there is an increase in both the energy cost and the specific electrolyzer investment cost due to the reduced efficiency (i.e., less hydrogen can be produced per installed kW).

3.4. Influence of electricity price

The magnitude of the energy cost penalty associated with direct electrochemical compression depends on the electricity price, which is the largest and most volatile cost component for the production of hydrogen from water electrolysis. In the present study, a relatively high electricity price of 0.12 € kWh^{-1} has been assumed (EU average in 2020), which only makes Case 1 and 2 (80 and 200 bar, respectively) economically viable. In Fig. 7 the LCOH has been plotted as a function of electricity price for the cases 1–3. Internal pressurization (dotted line) is compared to a combination of internal and external pressurization (solid line) and the intercepts indicate the electricity cost below which direct electrochemical compression may be economically viable. The intercepts are found at 0.40 € kWh^{-1} at 80 bar (not shown in Fig. 7), 0.16 € kWh^{-1} at 200 bar, and 0.09 € kWh^{-1} at 350 bar.

In order to compete with hydrogen from fossil-based SMR-processes today, the green hydrogen production cost needs to come down to around 2 € kgH_2^{-1} [57]. A prerequisite to reach this target is a low cost of renewable electricity. For the system considered in this study an electricity cost as low as 0.018 € kWh^{-1} would be required to be able to produce hydrogen at 2 € kgH_2^{-1}. With such low electricity costs, high-pressure electrolysis becomes much more favorable. At 200 bar the PEMEL system will, for example, now be able to accommodate a CAPEX increase of 330 € kW^{-1} (ca. 35%) and still be economically viable.

3.5. Sensitivity analyses

Figure 8 summarizes the results of the sensitivity analysis insvestigating the changes required in electricity price, PEMEL system CAPEX, compressor CAPEX, and compressor service rate to make direct compression economically equal to mechanical compression. The use cases 1–3 (80, 200, and 350 bar) are included in the analyis, highlighting the boundary conditions between which pressurized operation can be viable. The illustration shows that the 80 bar case will no longer be viable if either *i*) the energy cost is higher than 0.40 € kWh^{-1}, *ii)* the PEMEL system CAPEX is more than 1010 € kW^{-1}, *iii)* the compressor CAPEX is below 1400 € kW^{-1}, or *iv)* the extra compressor service cost each 5000 h of operation is removed entirely. As for the 200 bar case, this will no longer be viable if *i*) the energy cost is higher than 0.16 € kWh^{-1}, *ii)* the PEMEL system CAPEX is more than 990 € kW^{-1}, *iii)* the compressor CAPEX is below 3100 € kW^{-1}, or *iv)* the extra compressor service cost each 5000 h of operation is less than 13% of the compressor CAPEX. Finally, the 350 bar-case may become economically viable if *i*) the energy cost is lower than 0.09 € kWh^{-1}, *ii)* the PEMEL system CAPEX is below 730 € kW^{-1}, or *iii)* the compressor CAPEX is above 4800 € kW^{-1}.

In Fig. 9 a more general sensitivity analysis of the various factors contributing to the cost of hydrogen for Case 2 (200 bar) has been carried out. The Tornado plots shows that the results are most sensitive to the energy cost and electrolyser efficiency, followed by electrolyser CAPEX, discount rate, and electrolyser capacity factor. It can be seen that a reduced stack lifetime of 1 year compared to the base case does not have a significant impact on the overall LCOH. This is important because PEMEL durability is likely to be one of the major concerns related to the implementation of high-pressure PEMEL systems due to issues with, e.g., membrane and catalyst stability. Since the membrane thickness is the major PEMEL cell design parameter that influences the electrolyzer performance at different pressure levels, a separate analysis of the electrolyzer membrane is included in section 3.6.

3.6. Membrane consideration and optimization

For the membrane thickness and the resulting energy use in the electrolyzer stack, there is a compromise between area resistance (voltage efficiency) and low gas crossover (Faradaic efficiency). Hence, the membrane thickness can be optimized to minimize the energy penalty of hydrogen production at various electrolyzer outlet pressures. Fig. 10a) shows the energetically optimal membrane thickness as a function of the electrolyzer outlet pressure at a final delivery pressure of 700 bar, using commercially available Nafion membranes. In this example, the optimal membrane thickness increases from about 55 μm at 30 bar differential pressure, to more than 148 μm at 200 bar.

It should be noticed that the optimal membranes at electrolyzer operating pressures below 200 bar are considerably thinner than the commercially most widespread PEMEL membranes such as N117 (183 μm). The use of thick perfluoroalkyl sulfonic acid (PFSA) type membranes in PEMELs is the result of a compromise between resistance and mechanical robustness [35], as the main challenge associated with the use of thinner PFSA membranes is that they show issues with creep failure under the generation pressure required for electrolysis [10]. The development of thinner, robust membranes is, however, subject to rigorous research, and promising results have been shown from the testing of reinforced 60 μm thick PFSA membranes [10]. Recently, there have also been reported successful tests using $\leq$ 50 μm thick membranes with gas recombination catalyst layers and radical scavengers to slow down membrane thinning [58].

The effect of membrane optimization on system energy use and hydrogen production costs is illustrated in Fig. 10b), where the optimal membrane thickness is compared to N117. Since the N117 thickness is optimal for operation at 260 bar, the two cases converge at this point. At 30 bar, a 3.4 kWh kgH_2^{-1}decrease in energy use and 0.47 € kgH_2^{-1} cost reduction can be achieved. Here it should be noted that the H_2 content in the O_2 stream ranges from 3 vol% at 5 bar with a 32 μm thick membrane to 14% at 200 bar with a 150 μm thick membrane; the latter is well above LFL. In practical systems, it is necessary to integrate a gas recombiner in the stack so that the system can be operated safely.

Another interesting observation is that since the cost differential between systems utilizing N117 and systems with optimized membranes is so much larger at 30 bar (0.47 € kgH_2^{-1}) than at 80 bar (0.21 € kgH_2^{-1}) and 200 bar (0.01 € kgH_2^{-1}), there is no longer any potential cost savings by electrochemically compressing the gas directly at these delivery pressures. In order to make internal pressurization economical in systems with optimal membrane thicknesses, the electricity cost would need to come down to 0.09 € kWh^{-1} at 80 bar and to 0.05 € kWh^{-1} at 200 bar.

4. Conclusions

Increasing the operating pressure of water electrolyzers and thereby eliminating the need for external mechanical compression is one of the pathways to reduce the overall costs of renewable hydrogen and increase the reliability of electrolyzer plants. In this work, the energy

consumption and economic viability of operating PEM water electrolyzers at 80, 200, 350, and 700 bar were investigated in detail and compared to state-of-the-art PEM systems operating at 30 bar in combination with a mechanical compressor.

The following conclusions can be made:

- In all the use cases considered, self-pressurized electrolyzers give a higher overall energy consumption than electrolyzers operating at 30 bar in combination with a hydrogen compressor. This is because the compression losses in the electrolyzer are higher than the alternative mechanical compression energy.
- A significant reduction in CAPEX can be realized by removing the mechanical compressor. Hence, the economic viability of high-pressure PEM water electrolysis depends on *i)* the energy cost and *ii)* the CAPEX of the high-pressure PEMEL system.
- With a PEMEL system cost of 900 € kW^{-1} and a compressor cost of 3800 € kW^{-1}, high-pressure electrolysis at 80, 200, and 350 bar may become economically viable with electricity prices below 0.4, 0.16, and 0.09 € kWh^{-1}, respectively.
- With an electricity price of 0.12 € kWh^{-1} (EU average for non-household consumers in 2020), high-pressure electrolysis at 80 and 200 bar can become economically viable if the PEMEL system CAPEX increase is less than ca. 10% compared to state-of-the-art.
- To be able to produce renewable hydrogen at the target of 2 € kgH_2^{-1} (fossil fuel parity) the cost of electricity needs to be as low as 0.02 € kWh^{-1}. A 200 bar PEMEL system could in this case accommodate a CAPEX increase of 35% (from 900 to 1230 € kW^{-1}) and still be economically viable in comparison with the use of a mechanical compressor.
- Optimization of membrane thicknesses can further reduce the hydrogen production cost, but mainly for low-pressure conditions. If an optimized membrane thickness is used, the electricity price needs to be further reduced to make high-pressure PEMEL cost-effective (e.g., below 0.09 € kWh^{-1} at 80 bar).

In summary, the most promising use cases for high-pressure PEMEL are found at 80 and 200 bar. This fits well with the pressure requirements for several industrial hydrogen applications, such as green methanol production, transport and storage in the natural gas grid, gas storage in salt caverns, and ammonia production. The analysis demonstrates that if a market for such applications arises, 80- and 200 bar PEM electrolysis systems may become economically viable. Hence, the study also justifies further research on high-pressure PEMEL systems (e.g. 200 bar system at IFE), with the objective to increase efficiency and reduce costs.

CRediT authorship contribution statement

Ragnhild Hancke: Conceptualization, Formal analysis, Methodology, Software, Writing – original draft. **Thomas Holm:** Visualization, Writing – original draft. **Øystein Ulleberg:** Funding acquisition, Methodology, Supervision, Writing – review & editing.

Declaration of Competing Interest

The authors declare that they have no known competing financial interests or personal relationships that could have appeared to influence the work reported in this paper.

Acknowledgments

The authors gratefully acknowledge support from MoZEES, a Norwegian Centre for Environment-friendly Energy Research (FME), co-sponsored by the Research Council of Norway (project number 257653) and 37 partners from research, industry, and public sector. The authors also thank Janis Danebergs for contributing to the economic model development.

Appendix A:. Technical model

The electrochemical and mass transport relations used to simulate the current- and voltage efficiency of the PEMEL cell are presented in this appendix, and Table A1 summarizes the empirical input parameters utilized. The cell voltage is the sum of the Nernst voltage (U_N) and the kinetic, ohmic, and diffusion overvoltages (U_{kin}, $U_{ohm,}$ and U_{diff}). The Nernst potential is 1.23 V in a water electrolysis cell at standard conditions, but increases with temperature T and partial pressure P_i according to [13]:

$$U_N = U_{rev} + \frac{R\cdot T}{2\cdot F} ln\left(\frac{P_{H_2}\sqrt{P_{O_2}}}{{P_{ref}}^{3/2} a_{H_2O}}\right) \tag{A1}$$

where P_{ref} denotes the standard ambient pressure and a_{H2O} the activity of water (unity when liquid water is present at the electrodes). The reversible potential can be expressed by the empirical relation [59]:

$$U_{rev}(T, 1\ atm) = 1.5184 - 0.0015421\cdot T + 9.523\cdot 10^{-5}\cdot T\log T + 9,84\cdot 10^{-8}\cdot T^2$$

which is applicable to up to 18 bar pressure. To account for pressure effects, the reversible potential can be calculated from first principles according to:

$$U_{rev} = \frac{\Delta G}{2\cdot F} = \frac{((H_{H_2} + 0.5\cdot H_{O_2} - H_{H_2O}) - T(S_{H_2} + 0.5\cdot S_{O_2} - S_{H_2O}))}{2\cdot F} \tag{A2}$$

Here ΔG is the change in Gibbs free energy. *H(T)* and *S(T,P)* are the reaction enthalpy and entropy, respectively, which are thermophysical properties with tabulated values retrieved in *EES*.

The kinetic overvoltage, U_{kin}, is the sum of the activation barrier on the anode (η_{O_2}) and the cathode (η_{H_2}) which can be described by the respective exchange current densities, i_a^{ex} and i_c^{ex}. The exchange current density at the anode is by far the lowest, and the anodic overvoltage thus dominates the kinetic losses. The expression for the kinetic losses is derived from the Butler-Volmer reaction, and yields the following relation when assuming the backward reaction rate can be neglected:

$$U_{kin} = \eta_{O_2} + \eta_{H_2} = \frac{R\cdot T}{\alpha_a\cdot 2\cdot F} ln\left(\frac{i}{i_a^{ex}}\right) + \frac{R\cdot T}{\alpha_c\cdot 2\cdot F} ln\left(\frac{i}{i_c^{ex}}\right) \tag{A3}$$

where α_a and α_c are the charge transfer coefficients for the anode and cathode which is related to the symmetry of the activation (energy) barrier in the

gas evolution process and usually assumes a value between zero and unity.

The Ohmic overvoltage U_{ohm} represents losses that are caused by the resistance to the flow of electric current through the cell components (dominated by contact resistances) R_{el}, and the flow of protons through the membrane R_m. In accordance with Ohm's law, the ohmic polarization increases linearly with current density:

$$U_{\text{ohm}} = (R_{\text{el}} + R_m)\cdot I = R_\Omega \cdot I \tag{A4}$$

The total ionic/electronic cell resistance R_Ω is expressed in ohms. The transport properties of Nafion in its fully hydrated state are well known [32], and an established empirical relation [60] has been used to describe the Arrhenius-type proton conductivity, σ_m:

$$\frac{\delta_m}{R_m} = \sigma_m = 2.29\cdot exp\left(\frac{-7829}{R\cdot T}\right) \tag{A5}$$

where δ_m is the membrane thickness. The total ohmic resistance is often determined experimentally by so-called High-Frequency Resistance (HFR) measurements, and by subtracting the protonic contribution, R_{el} can be determined. Mass transport polarization, or diffusion overvoltage U_{diff}, is a non-Faradaic loss which is a function of the ratio of the pressure at the electrode interface to the pressure inside the channel:

$$U_{\text{diff,O}_2} = \frac{R\,T}{4\,F} ln\left(\frac{P_{\text{O}_2}}{P_{\text{O}_2,\text{ch}} - P_{\text{vp}}}\right) \tag{A6}$$

$$U_{\text{diff,H}_2} = \frac{R\,T}{2\,F} ln\left(\frac{P_{\text{H}_2}}{P_{\text{H}_2,\text{ch}} - P_{\text{vp}}}\right) \tag{A7}$$

Here $P_{\text{H2,ch}}$ and $P_{\text{O2,ch}}$ is the pressure measured inside the cathodic and anodic channels, resepctively, and P_{vp} is the vapor pressure of water which is calculated using the Tetens equation. In commercial PEMELs, the mass-transport limitation effect is hardly seen because the applied current densities are not high enough. It is generally recognized that the partial pressures of H_2 and O_2 inside the catalyst layers, P_{H_2} and P_{O_2}, will be higher than the measured pressure in the channels due to supersaturation in the layers. This pressure enhancement is proportional to the current density (i.e. gas production rate) and related by a partial pressure increase factor γ (bar cm^2 A^{-1}) [34]. The hydrogen pressure inside the cathode catalyst layer can be described as:

$$P_{\text{H}_2} = P_{\text{H}_2,\text{ch}} + \gamma_{\text{H}_2}\, i - P_{vp} \tag{A8}$$

The hydrogen partial pressure increase factor is an empirical parameter which depends on the structure, thickness, and permeability of the catalyst layer. Assuming that the anodic and cathodic catalyst layers have similar thicknesses and structures, the fit parameter for the partial pressure increase factor for oxygen in the anodic catalyst layer has been described by Schalenbach et al. [34]:

$$\gamma_{\text{O}_2} = \frac{\varepsilon_{\text{H}_2,\text{Fick}}}{\varepsilon_{\text{O}_2,\text{Fick}}}\cdot 0.5\cdot\gamma_{\text{H}_2} \tag{A9}$$

Here $\varepsilon_{i,Fick}$ is the diffusivity (mol cm^{-1} s^{-1} bar^{-1}) of species i in Nafion.

The gross hydrogen production rate $\dot{n}_{\text{H}_2}$ (mol cm^{-2} s^{-1}) is proportional to the current density according to Faraday's law:

$$\dot{n}_{\text{H}_2} = \frac{i}{2\cdot F} \tag{A10}$$

The cross-permeation flux density of hydrogen and oxygen can be derived based on Fick's law:

$$j_{H_2,Fick} = \varepsilon_{H_2,Fick}\cdot\left(\frac{\Delta P_{H_2}}{\delta_m}\right) \tag{A11}$$

$$j_{O_2,Fick} = \varepsilon_{O_2,Fick}\cdot\left(\frac{\Delta P_{O_2}}{\delta_m}\right) \tag{A12}$$

From Darcy's law, the cross-permeation flux of hydrogen by convection for higher cathodic than anodic absolute pressures can be represented as [13]:

$$j_{\text{H}_2,\text{Darcy}} = \varepsilon_{\text{H}_2,\text{Darcy}}\left(\frac{P_{\text{H}_2} - P_{\text{O}_2}}{\delta_m}\right) \tag{A13}$$

Where $\varepsilon_{\text{H}_2,\text{Darcy}}$ is the hydrogen permeability driven by Δp. Finally, the electro-osmotic drag of water during electrolysis contributes to the gas cross-permeation due to the solubility of H_2 and O_2 in water. This contribution to the cross-permeation is proportional to the empirical electro-osmotic drag coefficient, $n_{\text{H}_2\text{O,eo}}$ (the ratio of moles of water per moles of protons transported from the anode to the cathode) [33,34]:

$$j_{\text{H}_2,\text{drag}} = \dot{n}_{\text{H}_2\text{O,eo}}\cdot\left(\frac{P_{\text{H}_2,\text{c}}\cdot S_{\text{H}_2}}{C_{\text{H}_2\text{O}}}\right) \tag{A14}$$

$$j_{\text{O}_2,\text{drag}} = \dot{n}_{\text{H}_2\text{O,eo}}\cdot\left(\frac{P_{\text{O}_2,\text{a}}\cdot S_{\text{O}_2}}{C_{\text{H}_2\text{O}}}\right) \tag{A15}$$

Where S_i is the gas solubility (mol cm^{-3} bar^{-1}), and $C_{\text{H}_2\text{O}}$ is the concentration of water in Nafion (mol/L). Notably, the electro-osmotic drag effectively *reduces* the cross-permeation flux of hydrogen because the proton flux has the opposite direction. The resulting total hydrogen and oxygen cross-permeation flux densities can be expressed as:

Table A1
Empirical Parameters used in the PEMEL cell model.

Parameter	Value	Unit
i_a^{ex}	1.6×10^{-8} [31]	A cm^{-2}
i_c^{ex}	0.1 [31]	A cm^{-2}
α_{an}	0.8	
α_{cat}	0.5 [61]	
R_{el}	0.005 *	Ω cm^2
γ_{H_2}	2.4 [34]	bar cm^2A^{-1}
$\varepsilon_{H_2,Darcy}$	2.0×10^{-11} [34]	mol $cm^{-1}s^{-1}bar^{-1}$
$\varepsilon_{H_2,Fick}$	4.7×10^{-11} [34]	mol $cm^{-1}s^{-1}bar^{-1}$
$\varepsilon_{O_2,Fick}$	2.0×10^{-11} [32]	mol $cm^{-1}s^{-1}bar^{-1}$
$\varepsilon_{O_2,Darcy}$	2.0×10^{-11} [32]	mol $cm^{-1}s^{-1}bar^{-1}$
S_{H_2}	0.7×10^{-7} [34]	mol cm^{-3} bar^{-1}
S_{O_2}	0.8×10^{-7} [34]	mol cm^{-3} bar^{-1}
n_{eo}	3.5 [33]	mol H_2O (mol H^+)$^{-1}$
C_{H_2O}	40 [34]	mol L−1

*Estimated based on ref. [62,63].

$$j_{H_2,loss} = j_{H_2,Fick} + j_{H_2,Darcy} - j_{H_2,drag} \quad \text{(A16)}$$

$$j_{O_2,loss} = j_{O_2,Fick} + j_{O_2,drag} \quad \text{(A17)}$$

The water drag fluxes are found to be more than one order of magnitude lower than the fluxes associated with Fickian and hydraulic diffusion, and these contributions can therefore for all practical purposes be neglected.

References

[1] IEA, *The Future of Hydrogen, IEA, Paris*. 2019, IEA, Paris.
[2] Abdin Z, et al. Hydrogen as an energy vector. Renew Sustain Energy Rev 2020;120:109620.
[3] Weidner S, et al. Feasibility study of large scale hydrogen power-to-gas applications and cost of the systems evolving with scaling up in Germany, Belgium and Iceland. Int J Hydrogen Energy 2018;43(33):15625–38.
[4] Bhaskar A, Assadi M, Nikpey Somehsaraei H. Decarbonization of the iron and steel industry with direct reduction of iron ore with green hydrogen. Energies 2020;13(3):758.
[5] Liu W, et al. The production and application of hydrogen in steel industry. Int J Hydrogen Energy 2021;46(17):10548–69.
[6] Zang G, et al. Technoeconomic and life cycle analysis of synthetic methanol production from hydrogen and industrial byproduct CO2. Environ Sci Technol 2021;55(8):5248–57.
[7] Bellotti D, et al. Feasibility study of methanol production plant from hydrogen and captured carbon dioxide. J CO2 Util 2017;21:132–8.
[8] Moreno-Gonzalez M, et al. Carbon-neutral fuels and chemicals: Economic analysis of renewable syngas pathways via CO2 electrolysis. Energy Convers Manage 2021;244:114452.
[9] IRENA, *Green Hydrogen Cost Reduction: Scaling up Electrolysers to Meet the 1.5°C Climate Goal*. 2020, International Renewable Energy Agency: Abu Dhabi.
[10] Ayers KE, et al. Research advances towards low cost, high efficiency PEM electrolysis. ECS Trans 2010;33(1):3–15.
[11] Haryu E, Nakazawa K, Taruya K. Mechanical structure and performance evaluation of high differential pressure water electrolysis cell. Honda R&D Techn Rev 2011;23.
[12] Grigoriev SA, et al. High-pressure PEM water electrolysis and corresponding safety issues. Int J Hydrogen Energy 2011;36(3):2721–8.
[13] Schalenbach M, et al. Acidic or Alkaline? Towards a new perspective on the efficiency of water electrolysis. J Electrochem Soc 2016;163(11):F3197–208.
[14] Hancke R, Ulleberg Ø, Bujlo P. *High-Pressure PEM Water Electrolysis System*. in *EFCF2021*. 2021, July 28. Zenodo.
[15] Bellosta von Colbe J, et al. Application of hydrides in hydrogen storage and compression: achievements, outlook and perspectives. Int J Hydrogen Energy 2019;44(15):7780–808.
[16] Modi P, Aguey-Zinsou K-F. Room temperature metal hydrides for stationary and heat storage applications: a review. Front Energy Res 2021;9.
[17] El Kharbachi A, et al. Metal hydrides and related materials. Energy carriers for novel hydrogen and electrochemical storage. J Phys Chem C 2020;124(14):7599–607.
[18] Fischedick M, et al. Techno-economic evaluation of innovative steel production technologies. J Cleaner Prod 2014;84:563–80.
[19] Spreitzer D, Schenk J. Reduction of iron oxides with hydrogen—A review. Steel Res Int 2019;90(10):1900108.
[20] Dalena F, et al. Advances in methanol production and utilization, with particular emphasis toward hydrogen generation via membrane reactor technology. Membranes (Basel) 2018;8(4):98.
[21] Djewels. *Project Description*. [cited 2021 13. Dec]; Available from: https://djewels.eu/project-description/].
[22] Jo Y, Ahn B. Analysis of hazard area associated with hydrogen gas transmission pipelines. Int J Hydrogen Energy 2006;31(14):2122–30.
[23] Giddey S, Badwal SPS, Kulkarni A. Review of electrochemical ammonia production technologies and materials. Int J Hydrogen Energy 2013;38(34):14576–94.
[24] Lord AS, Kobos PH, Borns DJ. Geologic storage of hydrogen: Scaling up to meet city transportation demands. Int J Hydrogen Energy 2014;39(28):15570–82.
[25] Crotogino F. Chapter 20 - Larger Scale Hydrogen Storage. In: Letcher TM, editor. Storing Energy. Oxford: Elsevier; 2016. p. 411–29.
[26] *Hydrogen Delivery Technical Team Roadmap*. 2013, US Department of Energy: Office of Energy Efficiency & Renewable Energy.
[27] Rose PK, Neumann F. Hydrogen refueling station networks for heavy-duty vehicles in future power systems. Transp Res Part D: Transp Environ 2020;83:102358.
[28] Nguyen T, et al. Grid-connected hydrogen production via large-scale water electrolysis. Energy Convers Manage 2019;200:112108.
[29] Talebian H, Herrera OE, Mérida W. Spatial and temporal optimization of hydrogen fuel supply chain for light duty passenger vehicles in British Columbia. Int J Hydrogen Energy 2019;44(47):25939–56.
[30] El-Emam RS, Özcan H. Comprehensive review on the techno-economics of sustainable large-scale clean hydrogen production. J Cleaner Prod 2019;220:593–609.
[31] Harrison KW, et al. Semiempirical model for determining PEM electrolyzer stack characteristics. J Fuel Cell Sci Technol 2006;3(2):220–3.
[32] Ito H, et al. Properties of Nafion membranes under PEM water electrolysis conditions. Int J Hydrogen Energy 2011;36(17):10527–40.
[33] Medina P, Santarelli M. Analysis of water transport in a high pressure PEM electrolyzer. Int J Hydrogen Energy 2010;35(11):5173–86.
[34] Schalenbach M, et al. Pressurized PEM water electrolysis: efficiency and gas crossover. Int J Hydrogen Energy 2013;38(35):14921–33.
[35] Babic U, et al. Critical review-identifying critical gaps for polymer electrolyte water electrolysis development. J Electrochem Soc 2017;164(4):F387–99.
[36] Kim H-S, et al. High efficiency isolated bidirectional AC-DC power converter. Berlin, Heidelberg: Springer Berlin Heidelberg; 2013.
[37] Onda K, et al. Prediction of production power for high-pressure hydrogen by high-pressure water electrolysis. J Power Sources 2004;132(1):64–70.
[38] Villagra A, Millet P. An analysis of PEM water electrolysis cells operating at elevated current densities. Int J Hydrogen Energy 2019;44(20):9708–17.
[39] Colella WG, James BD, Moton JM. *Techno-economic Analysis of PEM Electrolysis for Hydrogen Production* in *Electrolytic Hydrogen Production Workshop*. 2014: NREL, Golden, Colorado.
[40] Huang P. Humidity standard of compressed hydrogen for fuel cell technology. ECS Trans 2008;12(1):479–84.
[41] Hollingsworth J, et al. *Chapter 5 - Reciprocating Compressors*, in *Compression Machinery for Oil and Gas*, K. Brun and R. Kurz, Editors. 2019, Gulf Professional Publishing. p. 167-252.
[42] *Addendum to the Multi-Annual Work Plan 2014 - 2020*, in *FUEL CELLS and HYDROGEN 2 JOINT UNDERTAKING (FCH 2 JU)*. 2018.
[43] Suermann M, Bensmann B, Hanke-Rauschenbach R. Degradation of Proton Exchange Membrane (PEM) water electrolysis cells: looking beyond the cell voltage increase. J Electrochem Soc 2019;166(10):F645–52.
[44] Saba SM, et al. The investment costs of electrolysis – A comparison of cost studies from the past 30 years. Int J Hydrogen Energy 2018;43(3):1209–23.
[45] Proost J. State-of-the art CAPEX data for water electrolysers, and their impact on renewable hydrogen price settings. Int J Hydrogen Energy 2019;44(9):4406–13.

[46] Chardonnet C, et al., *Study on Early Business Cases for H2 in Energy Storage and More Broadly Power to H2 Applications*. 2017, FCH JU.
[47] Ulleberg Ø, Hancke R. Techno-economic calculations of small-scale hydrogen supply systems for zero emission transport in Norway. Int J Hydrogen Energy 2020;45(2):1201–11.
[48] Ulleberg Ø, et al. *Hynor Lillestrøm – A Renewable Hydrogen Station & Technology Test Center*, in *20th World Hydrogen Energy Conference*. South Korea: Gwangju Metropolitan City; 2014.
[49] Seyboth K, et al., *Renewable Energy Sources and Climate Change Mitigation Special Report of the Intergovernmental Panel on Climate Change*, O. Edenhofer, R.P. Madruga, and Y. Sokona, Editors. 2011, Intergovernmental Panel on Climate Change: Cambridge University Press.
[50] Eurostat. *Electricity price statistics, first half 2021*. [cited 2021 13. Dec]; Available from: https://ec.europa.eu/eurostat/statistics-explained/index.php?title=Electricity_price_statistics].
[51] Eurostat. *Renewable energy statistics*. [cited 2021 13. Dec]; Available from: https://ec.europa.eu/eurostat/statistics-explained/index.php?title=Renewable_energy_statistics].
[52] Statnett. *This year's tariff*. [cited 2021 13. Oct]; Available from: https://www.statnett.no/en/for-stakeholders-in-the-power-industry/tariffs/this-years-tariff/].
[53] Sartory M, et al. Theoretical and experimental analysis of an asymmetric high pressure PEM water electrolyser up to 155 bar. Int J Hydrogen Energy 2017;42(52):30493–508.
[54] Suermann M, Schmidt TJ, Buchi FN. Cell performance determining parameters in high pressure water electrolysis. Electrochim Acta 2016;211:989–97.
[55] Bensmann B, et al. Optimal configuration and pressure levels of electrolyzer plants in context of power-to-gas applications. Appl Energy 2016;167:107–24.
[56] Tjarks G, et al. Energetically-optimal PEM electrolyzer pressure in power-to-gas plants. Appl Energy 2018;218:192–8.
[57] Proost J. Critical assessment of the production scale required for fossil parity of green electrolytic hydrogen. Int J Hydrogen Energy 2020;45(35):17067–75.
[58] Park A. *Performance and Durability Investigation of Thin, Low Crossover Proton Exchange Membranes for Water Electrolyzers*, in *2020 Annual Merit Review: Progress Updates*. 2020, Department of Energy.
[59] LeRoy RL, Bowen CT, LeRoy DJ. The thermodynamics of aqueous water electrolysis. J Electrochem Soc 1980;127(9):1954–62.
[60] Kopitzke RW, et al. Conductivity and water uptake of aromatic-based proton exchange membrane electrolytes. J Electrochem Soc 2000;147(5):1677–81.
[61] Garcia-Valverde R, Espinosa N, Urbina A. Simple PEM water electrolyser model and experimental validation. Int J Hydrogen Energy 2012;37(2):1927–38.
[62] Bernt M, Gasteiger HA. Influence of ionomer content in IrO2/TiO2 electrodes on PEM water electrolyzer performance. J Electrochem Soc 2016;163(11):F3179–89.
[63] Suermann M, et al. High pressure polymer electrolyte water electrolysis: test bench development and electrochemical analysis. Int J Hydrogen Energy 2017;42(17):12076–86.